Water Resources Research

RESEARCH ARTICLE
10.1029/2020WR027282

The Stream Length Duration Curve: A Tool for Characterizing the Time Variability of the Flowing Stream Length

G. Botter[1] and N. Durighetto[1]

[1]Department of Civil, Environmental and Architectural Engineering, University of Padua, Padua, Italy

Key Points:
- The concept of Stream Length Duration Curve is formalized and applied to a real-world case study
- Stochastic models are developed to link the Stream Length Duration Curve to the network structure and local hydrological properties
- In the Valfredda catchment (Italy), the activation of temporary reaches follows a hierarchical order

Supporting Information:
- Supporting Information S1

Correspondence to:
N. Durighetto,
nicola.durighetto@gmail.com

Citation:
Botter, G., Durighetto, N. (2020). The Stream Length Duration Curve: A tool for characterizing the time variability of the flowing stream length. *Water Resources Research*, *56*, e2020WR027282. https://doi.org/10.1029/2020WR027282

Received 12 FEB 2020
Accepted 13 JUL 2020
Accepted article online 17 JUL 2020

Abstract In spite of the importance of stream network dynamics for hydrology, ecology, and biogeochemistry, there is limited availability of analytical tools suitable for characterizing the temporal variability of the active fraction of river networks. To fill this gap, we introduce the concept of Stream Length Duration Curve (SLDC), the inverse of the exceedance probability of the total length of active streams. SLDCs summarize efficiently the effect of hydrological variability on the length of the flowing streams under a variety of settings. A set of stochastic network models is developed to link the features of the local hydrological status of the network nodes with the shape of the SLDC. We show that the mean network length is dictated by the mean persistency of the nodes, whereas the shape of the SLDC is driven by the spatial distribution of the local persistencies and their network-scale spatial correlation. Ten field surveys performed in 2018 were used to estimate the empirical SLDC of the Valfredda river (Italy), which was found to be steep and regular—indicating a pronounced sensitivity of the active stream length to the underlying hydrological conditions. Available observations also suggest that the activation of temporary reaches during network expansion is hierarchical, from the most to the least persistent stretches. Under these circumstances, the SLDC corresponds to the spatial Cumulative Distribution Function of the nodes persistencies. The study provides a sound theoretical basis for the analyses of network dynamics in temporary rivers.

1. Introduction

A significant fraction of the global river network includes temporary streams—that is, streams that are active only during certain seasons of the year or after precipitation events (Downing et al., 2012; Skoulikidis et al., 2017; Tooth, 2000). Intermittent streams are observed across a variety of climatic settings, from the humid headwater catchments in the Alps or North-Eastern United States to semiarid regions, where most rivers experience flow only episodically. Intermittent and ephemeral rivers are especially valuable as they support a unique high-biodiversity and, therefore, require the development of ad hoc classification and monitoring strategies (McDonough et al., 2011; Skoulikidis et al., 2017) that would benefit from the development of general statistical tools for the characterization of active stream network dynamics.

In spite of the recognized ecological and hydrologic relevance of stream dynamics, historically river networks have been long considered as static components of catchments. In the last years, however, temporary and ephemeral streams have gained increasing attention from the scientific community. Many experimental studies have been conducted in different regions of the World to quantify event-based and seasonal dynamics of the active stream network (Agren et al., 2015; Blyth & Rodda, 1973; Day, 1978; Datry et al., 2016; Doering et al., 2007; Durighetto et al., 2020; Godsey & Kirchner, 2014; Goulsbra et al., 2014; Gregory & Walling, 1968; Jaeger et al., 2007; Jensen et al., 2017, 2019; Lovill et al., 2018; Malard et al., 2006; Peirce & Lindsay, 2015; Roberts & Klingeman, 1972; Shaw, 2016; Shaw et al., 2017; van Meerveld et al., 2019; Whiting & Godsey, 2016; Zimmer & McGlynn, 2017). These field surveys revealed that stream network expansion/contraction generated by climate variability represents a general rule rather than an exception, and a major fraction of the existing drainage network is, in most circumstances, dynamical (e.g., Datry et al., 2014).

The implications of stream dynamics extend far beyond hydrology. The shape and the length of the active stream network, in fact, represents a key determinant of a variety of ecological and biogeochemical processes such as biological dispersion, nutrient spiraling and CO_2 outgassing (e.g., Arthington et al., 2014; Basu et al.,

2011; Bernal & Sabater, 2008; Bertuzzo et al., 2017; Botter et al., 2007; Butturini et al., 2008; Datry et al., 2017; Garbin et al., 2019; Jaeger et al., 2014; Larned et al., 2010; Marzadri et al., 2017; Peterson et al., 2001; Steward et al., 2012; Sarremejane et al., 2017). Therefore, an objective quantification of the time variability of the active stream length across scales is recognized as a key issue in biogeochemistry and environmental sciences (Costigan et al., 2016; Datry et al., 2014).

In spite of the improved insight on the major causes and consequences of stream network dynamics, to date there is a limited availability of analytical tools with general applicability that are suitable to objectively characterize the magnitude and the extent of river network variability through time. To date, the outcome of experimental surveys is usually represented by a set of active stream network maps characterized by different scales and resolutions (e.g., Jensen et al., 2018; Shaw et al., 2017), complemented by a variety of statistical analyses of relevant stream attributes (e.g., stream length, discharge, number of flow origins, and connectivity). Consequently, due to the heterogeneity of the available data sets, comparative analyses and quantitative syntheses of the observed patters of river network dynamics across different geographic areas are lacking. On the other hand, currently available definitions of ephemeral and intermittent water courses are often qualitative (e.g., Datry et al., 2016; Jensen et al., 2017; Wiginton et al., 2005). Therefore, comparative studies would be helpful for the development of general criteria for the classification of temporary watercourses and the identification of targeted policy actions.

With the above premises, in this paper we address the following major research question: how can stream network dynamics be efficiently and objectively characterized regardless of the specific conditions (e.g., temporal resolution, catchment size, and climatic regime) under which empirical surveys were carried out? To fill this gap we introduce the concept of Stream Length Duration Curve (SLDC), which is inspired by the analogous hydrological concept of Flow Duration Curve. SLDCs are proposed as a general tool to quantify the natural temporal variability of the active stream network under a broad range of field settings. Moreover, we combine theoretical analyses and field data to address the following additional issues: (i) What is the link between the features of the local hydrological status of the network nodes and the shape of the SLDC? (ii) Does the activation of temporary river stretches in intermittent rivers follow some identifiable order?

These research questions are tackled exploiting a statistical approach that allows the identification of a set of objective metrics for the characterization of stream network dynamics. In particular, we focus here on the main statistics of the total active length, and we relate these key network-scale properties to measurable, local hydrological features such as the persistency of the network nodes and the underlying spatial correlations. The combination of analytical tools, numerical simulations, and empirical data employed in this paper elucidates the main physical and statistical drivers that control active length variations in temporary streams. An overview of the major implications for processes understanding and stream network modeling/monitoring is also provided.

2. Theory

2.1. Theoretical Framework

Let us define a dynamical stream network through a set of N nodes with arbitrary spatial coordinates within a 3-D space, representative of the terrain of a given landscape. In this framework, the dynamical nature of the stream network can be probabilistically represented by a random shifting between two possible states associated to each node: "active" or "dry." From a mathematical viewpoint, the river network thus corresponds to a vector of N binary random variables $\mathbf{X} = (X_1, X_2, \dots, X_N)$, whose components are associated to the N nodes of the network. Specifically, X_k ($k \in (1, N)$) characterizes the local status of the kth node according to the following coding scheme:

$$X_k = \begin{cases} 0 & \text{if the node is dry} \\ 1 & \text{if the node is active} \end{cases}. \quad (1)$$

X_k follows a Bernoulli probability distribution with parameter p_k:

$$X_k \sim p_k^{x_k} \left(1 - p_k\right)^{1 - x_k}, \tag{2}$$

where x_k denotes a realization of the stochastic variable X_k and the symbol $\sim$ means "is distributed as." The mean and the variance of the dichotomic process at the node k, X_k, can be expressed as

$$E[X_k] = p_k$$

$$E[(X_k - E[X_k])^2] = p_k(1 - p_k),$$

where $E[...]$ denotes expectation. Therefore, the parameter p_k in Equation 2 represents the mean local persistency of the node k (i.e., the average percentage of time during which the node k is active). The mean local persistency (hereafter local persistency) can be estimated from independent field surveys as the sample mean of X_k, that is, $p_k = \frac{Na_k}{N_k} \in [0; 1]$, where Na_k is the number of surveys in which the node k is active and N_k the number of times the node k was surveyed (see, e.g., Durighetto et al., 2020). It is worth noting that the quantity p_k is a local property in space, though temporally integrated.

The length of the active stream network at a given time is crucially dependent on two independent factors, namely, (i) the fraction of stream length associated to each node and (ii) the sequence of nodes active at a given time. In particular, the stream network length L can be expressed as

$$L = \mathbf{X} \cdot \Delta l, \tag{3}$$

where $\cdot$ indicates the scalar product and $\mathbf{\Delta}\, l$ is a vector of lengths—$\mathbf{\Delta}\, l = (\Delta l_1, \Delta l_2, \ldots, \Delta l_N)$—whose components represent the increase of overall stream length produced by the activation of each node of the network. Δl_k can be calculated (for every node) based on the network topology as the sum of the semidistances between the node at hand and the connected neighboring nodes (upstream and downstream), suitably evaluated along the flow directions. Equation 3 shows that, due to the randomness of $\mathbf{X}$, the active stream network length is a random variable as well.

The sequence of nodes that are active at a given time can be characterized in a probabilistic way through the definition of the joint pdf of the vector of N random variables $X_k, k \in [1, N]$. The joint pdf of the random vector $\mathbf{X}$ is a multivariate Bernoulli distribution, with possibly correlated components. The analytical expression of this multivariate distribution reads (e.g., Dai et al., 2013)

$$p(\boldsymbol{x}) = p_{00\ldots0}^{\left[\prod_{j=1}^{N}(1 - x_j)\right]} p_{10\ldots0}^{\left[x_1 \prod_{j=2}^{N}(1 - x_j)\right]} p_{01\ldots0}^{\left[(1 - x_1)x_2 \prod_{j=3}^{N}(1 - x_j)\right]} \ldots p_{11\ldots1}^{\left[\prod_{j=1}^{N} x_j\right]} \tag{4}$$

where $p_{abc..z}$ is the joint probability of $X_1 = a$, $X_2 = b$, $X_3 = c$, $\ldots$, $X_N = z$ and $\mathbf{x} = (x_1, x_2, \ldots, x_N)$ represents a realization of $\mathbf{X}$. In order to fully specify the joint pdf in Equation 4, the identification of a large number of parameters (2^N) is required. Therefore, the problem can be largely undetermined (i.e., overparametrized) unless further simplifying assumptions are introduced.

The mean network length can be calculated based on the local persistency, taking the expectation of both sides of Equation 3:

$$\langle L \rangle = \sum_{i=1}^{N} p_i \, \Delta l_i. \tag{5}$$

Equation 5 shows that the mean length can be expressed as a weighted sum of the local persistency along the network. Nevertheless, changes in the state (active vs. dry) of the nodes of the network, as induced by the interaction of unsteady climatic forcing (e.g., a random sequence of rainfall events) and local geologic or morphological properties, make the overall length of the flowing streams time variable. The variability in time of the stream network length can be summarized through the variance of L that can be estimated from Equation 3 as the variance of a linear combination of random variables:

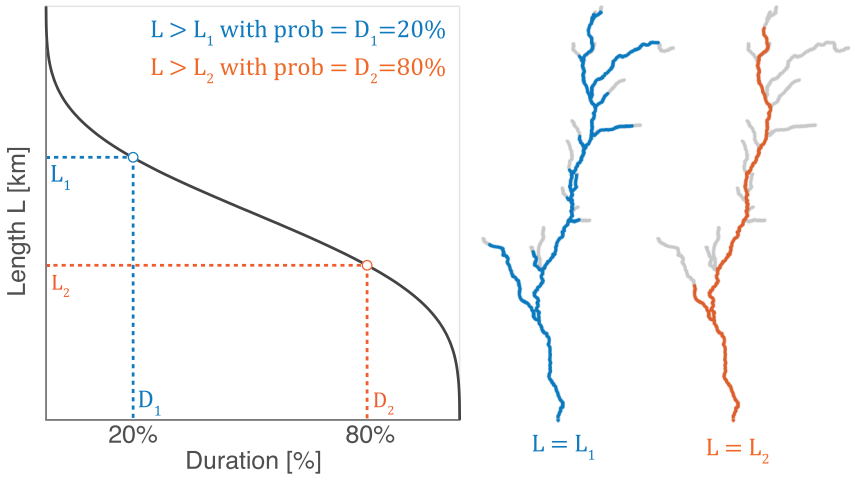

Figure 1. Schematic of a Stream Length Duration Curve.

$$var(L)=\sum_{i=1}^{N}\sum_{j=1}^{N}\Delta l_i \Delta l_j Cov(X_i, X_j)=\sum_{i=1}^{N}\sum_{j=1}^{N}\rho_{i,j}\Delta l_i \Delta l_j \sqrt{p_i(1-p_i)p_j(1-p_j)}, \quad (6)$$

where $Cov(X_i, X_j)$ is the covariance between X_i and X_j and $\rho_{i,j}$ is the corresponding cross correlation (i.e., the covariance scaled to the product of the standard deviations of X_i and X_j). Equation 6 shows that, differently from the mean network extension, the variability of the stream length through time is crucially impacted by the spatial correlation structure of the sequence of random states X_k along the network.

The temporal variability of the length of the flowing streams can be characterized in a more detailed manner through the probability density function (pdf) of L—or, alternatively, through the corresponding Cumulative Distribution Functions (CDFs) of L (exceedance or nonexceedance probabilities). A general closed-form expression for the exceedance probability of the length of the flowing network, $P_L(L)$, can be written as

$$P_L(L)=Prob\ [l \geq L]=Prob\ [\mathbf{X}\cdot\boldsymbol{\Delta}l \geq L]. \quad (7)$$

The left-hand side of Equation 7 represents the probability to observe a length of flowing streams larger than (or equal to) L, while the right-hand side of the same equation represents the CDF of a linear combination of possibly correlated Bernoulli-distributed binary random variables. Were these binary variables uncorrelated, the pdf of the stream length would be expressed as a convolution of N scaled Bernoulli pdfs, thereby originating a Binomial-Bernoulli distribution when $\Delta l_k = const(k)$. Instead, the presence of mutual correlations among the components of $\mathbf{X}$, which is a reflection of the physical mechanisms that underlie river network expansion and contractions, prevents a full analytical treatment of the problem in the general case, unless further simplifying assumptions are introduced (see section 2.3).

Being a monotonic function of L, the exceedance probability of the active stream length, $P_L(L)$, can be inverted and reinterpreted as the active SLDC, in analogy with the definition of flow duration curve that is widely employed in the hydrological literature and in practical engineering to characterize the temporal variability of the flow rate at a station (e.g., Castellarin et al., 2004; Doulatyari et al., 2015; Vogel & Fennessey, 1994). This can be done graphically by putting all the possible active flow lengths (L) on the y axis of a plot and then representing on the x axis the corresponding percentage of time, $D(L)$, for which that specific length is equalled or exceeded (Figure 1). This produces a function $L(D)$ that is the inverse of the exceedance probability of the active stream length given by Equation 7. By construction, the area underlying the SLDC represents the mean length of the active streams, as given by Equation 5, while the slope of the SLDC is proportional to the variance of L expressed by Equation 6.

As discussed above, the shape of the SLDC is a reflection of the degree of temporariness of the various nodes of the network and the correlations among the states of the nodes. Understanding how all these factors are

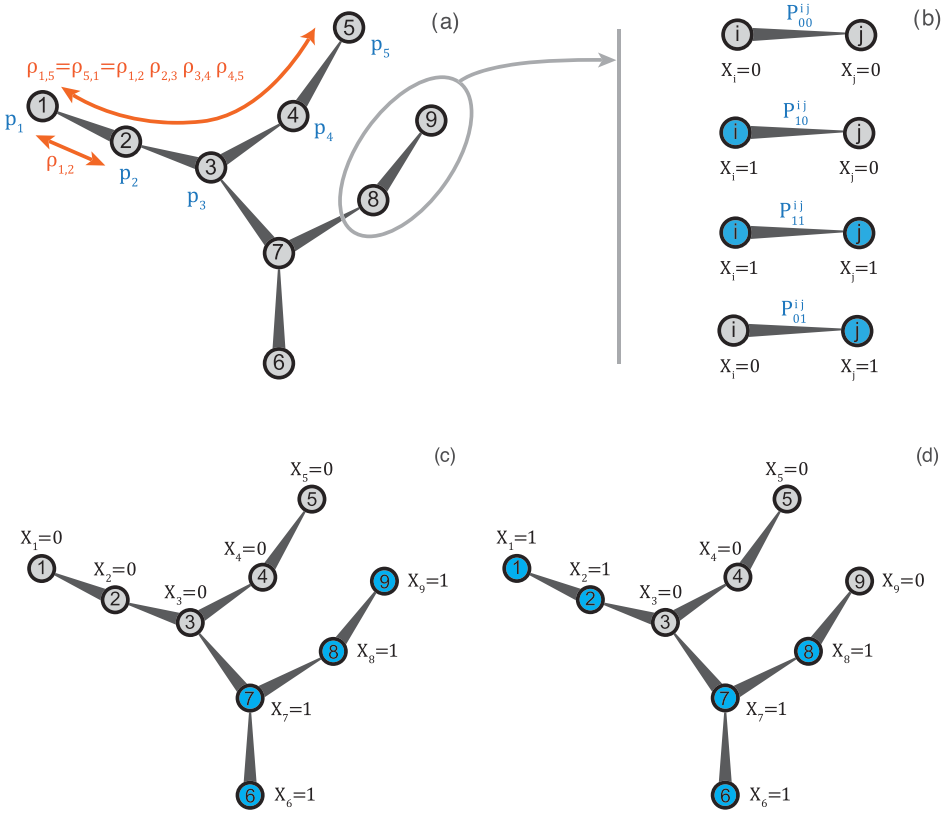

Figure 2. (a) Schematic of a Bayesian binary network with two possible states (active or dry). Each node, represented by a circle, is identified by a number. Nodes are linked together by directed edges to represent the dependence structure of the network. Blue labels represent marginal probabilities of node activation; orange labels indicate the correlation between two nodes. (b) Schematic of the joint probability of activation of two connected nodes *i* and *j*, as indicated by the blue labels. Active nodes ($X = 1$) are color coded as blue, while dry nodes ($X = 0$) are represented in gray. (c and d) Two example configurations of possible states of the nodes. The active nodes may or may not be continuous along the network.

mirrored by the shape of the SLDC and the corresponding time variability of the active stream network length is one of the major goals of this study.

2.2. A Bayesian Model of Stream Network Dynamics

Given the complexity of the physical processes under investigation, a simplified probabilistic description of the nodes state in the network can be helpful to quantify the effect of the expansion/contraction cycles experienced by rivers on the temporal variability of the active stream length. Here, stream network dynamics are described through a spatially correlated dichotomic stochastic process, in which the state of one node is seen as a binary random variable (active/dry, see Equation 1) that is probabilistically linked to the state of another (suitably identified) node in the network. In other words, pairwise joint pdfs representing the status of two connected nodes are identified (Figure 2). If we now consider a generic couple of directly connected nodes (say, the nodes *j* and *i*), the joint probabilities of the state of these nodes are identified by the following elements (Figure 2):

- p^{ji}_{11} (probability that the node *j*is active and the node *i*is active);
- p^{ji}_{10} (probability that the node *j*is active and the node *i*is dry);
- p^{ji}_{01} (probability that the node *j*is dry and the node *i*is active);
- p^{ji}_{00} (probability that the node *j*is dry and the node *i*is dry);

(8)

These joint pdfs are spatially variable (i.e., they do depend on the couple of nodes at hand, as reflected by the notation) and must obey to the following additional constraints: $p_{11}^{ji} + p_{10}^{ji} = p_j$, $p_{01}^{ji} + p_{11}^{ji} = p_i$, and $p_{11}^{ji} + p_{10}^{ji} + p_{01}^{ji} + p_{00}^{ji} = 1$ (joint and marginal pdfs must be consistent, and the total probability has to be conserved). A few important remarks are in order: (i) This is a probabilistic model, and mechanistic cause-effect relationships affecting the sequential activation of different nodes are not necessarily represented in an explicit manner; (ii) the pairs of connected nodes are not necessarily close-by in the physical space (the probabilistic space and the geometric space are different); (iii) assuming a direction in the connections between any pair of nodes is necessary for the calculation of pairwise conditional pdfs and, thus, for the calculation of the joint pdf of the node states according to the Bayesian paradigm. The directionality of the links allows the identification of a parent and a child node for each pair of connected nodes, such as the connection is directed from the parent to the child. However, these directions might be arbitrary (i.e., they can be reversed provided that only pairwise conditional pdfs are generated) and do not necessarily reflect causality (see Point (i) above). Under the above assumptions, the correlation between two directly connected nodes X_i and X_j, ρ_{ij} reads

$$\rho_{i,j} = \frac{p_{11}^{ji} - p_i\, p_j}{\sqrt{p_i\, p_j (1 - p_i)(1 - p_j)}}. \tag{9}$$

The correlation ρ given above quantifies the probability that two neighboring nodes are simultaneously active or simultaneously dry. Nevertheless, the correlation can be calculated for both neighboring and non-neighboring nodes. The correlation between two nodes k and m that are not directly connected can also be expressed as

$$\rho_{k,m} = \prod_{i:k->m} \rho_{i,i+1}, \tag{10}$$

where the product involves all the couples of directly connected nodes $(i,i+1)$ that generate a path connecting the nodes k and m (see Figure 2). Therefore, the full correlation structure of the network is identified by the pairwise correlations of the states of neighboring nodes (hereafter, local correlations). Overall, a dichotomic Bayesian network is thus defined through the specification of five attributes: (i) the number of nodes N, (ii) the stream length associated to each node (i.e., the vector $\mathbf{\Delta}\, l$), (iii) the network structure, that is, how each node is connected with the other nodes, (iv) the N local persistencies p_i, and (v) the $N-1$ local spatial correlations between neighboring nodes, $\rho_{i,j}$. The mean degree of correlation of the network, $\langle \rho_{ntwk} \rangle$, can be then calculated as

$$\langle \rho_{ntwk} \rangle = \frac{1}{N^2} \sum_{k=1}^{N} \sum_{m=1}^{N} \rho_{k,m}. \tag{11}$$

Equation 11 expresses the overall correlation of the system as the average correlation existing among all the possible couples of (directly or indirectly) connected nodes of the network. The $\langle \rho_{ntwk} \rangle$ is a lumped measure of the degree of spatial correlation of the random states $\mathbf{X}$ within a temporary stream.

A key element of the formulation is that the correlation between two nodes is constrained by the local persistence of the two nodes. In fact, for a given couple of nodes i,j with local persistencies p_i and $p_j \le p_i$, the maximum possible correlation between the nodes, ρ_{ij}^{max}, is

$$\rho_{i,j}^{max} = \sqrt{\frac{p_j(1 - p_i)}{p_i(1 - p_j)}} \le 1, \tag{12}$$

while the corresponding minimum possible correlation, ρ_{ij}^{min}, reads

$$\rho_{i,j}^{min} = -\left(\frac{p_i p_j}{(1 - p_i)(1 - p_j)} \right)^{\beta} \ge -1, \tag{13}$$

where $\beta = 1/2$ if $p_i + p_j \le 1$ and $\beta = -1/2$ otherwise. Therefore, the full set of possible correlations (i.e., the range $(-1, 1)$) is available only when $p_i = p_j = 0.5$. Otherwise, the maximum local correlation is upwardly bounded or the minimum correlation is downwardly bounded. For example, two nodes with persistency 0.5 can display a correlation between -1 and 1, two nodes with persistency 0.9 have a correlation

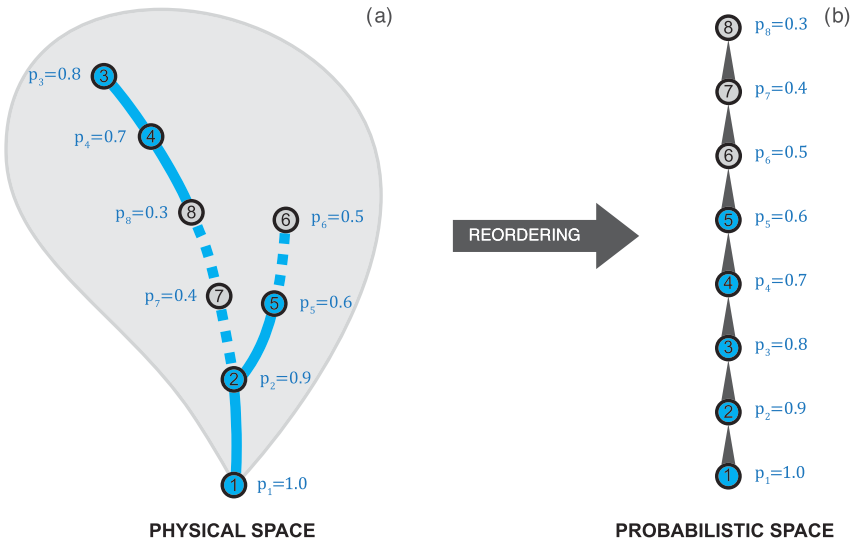

Figure 3. Schematic of the hierarchical model applied to an example river network with eight nodes. (a) A representative stream network drawn as a blue line that can be either active (continuous) or dry (dotted line). The nodes are active (blue) or dry (gray) accordingly. (b) Schematic of the corresponding chain obtained by applying the hierarchical model. The nodes are first reordered from the most to the least persistent and then direct connections between nodes are set. If the condition $p_{01}^{(i-1)\ i}=0$ is set for all the neighboring nodes, then node activation follows the chain order (i.e., Node 1 is the first to be activated, while Node 8 is active only when all the other nodes are already switched on). Note that the reordering of the nodes allows the hierarchical model to describe also active stream networks that are discontinuous in the physical space.

between −0.11 and 1, whereas for two nodes with persistencies (0.1,0.9) the correlation ranges between −1 and 0.11. In the supporting information we show the lower and upper limits of the local correlation as a function of the underlying persistencies. It is worth mentioning that a unit linear Pearson correlation is possible only in the case of $p_i = p_j$, for which two connected nodes can be systematically active at the very same time. As one of the two local persistencies of the connected nodes (or both) tend to 0 or 1, the upper limit of the local correlation approaches 0. The implications of these correlation limits on the shape of the SLDC will be discussed in the following sections.

2.3. A Persistency-Driven Hierarchical Model of Stream Network Dynamics

In this section, we describe a simplified case of the model presented in section 2.2, in which the switching on of the various network's nodes during the expansion of the flowing streams takes place in a hierarchical way —from the most persistent to the least persistent nodes. Mathematically, this implies that the nodes are first reordered in a chain based on their local persistency, from the most to the least persistent (Figure 3). Then pairwise connections are set between consecutive nodes (i.e., between the nodes $i-1$ and i) imposing the constraint $p_{01}^{(i-1)\ i}=0$ (in which the first subscript refers to the status of the most persistent node of the pair, and the second subscript refers to the state of the least persistent) for all the possible pairs of directly connected nodes. This does not imply that the underlying active stream network is spatially continuous, as the reordering does not reflect the actual position of the nodes (two connected nodes can be far apart in the physical space, as in the example of Figure 3). Under these assumptions, the three nonnull joint pdfs defined in Equation 8 can be written as

$$\begin{aligned} p_{11}^{(i-1)\ i} &= p_i - p_{01}^{(i-1)\ i} = p_i \\ p_{10}^{(i-1)\ i} &= p_{i-1} - p_{11}^{(i-1)\ i} = p_{i-1} - p_i \\ p_{00}^{(i-1)\ i} &= (1-p_{i-1}) - p_{01}^{(i-1)\ i} = 1 - p_{i-1}, \end{aligned} \tag{14}$$

where the nodes i and $i-1$ are two consecutive nodes in the chain, reordered by descending persistency (i.e., $p_i < p_{i-1}$).

This process represents a single chain, in which all the nodes with the same local persistency (i.e., same p_i) behave systematically in the same manner (they are all simultaneously switched on or switched off). Moreover, a node with a given p_i can be switched on only if all the network's nodes with a larger local persistency are already switched on. In this case, a mechanistic relationship between pairs of nodes is introduced as the switching on of the $i-1$ node is a necessary (but not sufficient) condition for the activation of the node i. The physical interpretation of this model is based on the idea that, during the network expansion, a hydrological signal is propagated along the network when a given landscape portion becomes saturated and, consequently, overland flow is generated.

Provided that the nodes are reordered according to a decreasing value of local persistency, each of the possible sequences of ordered nodes corresponds to a sequence of K ($K \in [0,1,2,\dots,N]$) active nodes ($X_1 = 1, X_2 = 1, \dots, X_k = 1$), followed by a sequence of $N-K$ dry nodes ($X_{K+1} = 0, X_{K+2} = 0, \dots, X_N = 0$). Accordingly, in Equation 4, the only nonzero terms of the joint pdf of $\mathbf{X}$ are those of the type $p_{1000,\dots,00}$, $p_{1100,\dots,00}$, $p_{1110,\dots,00}$, ..., $p_{1111,\dots,10}$, $p_{1111\dots11}$ and a single transition from 1 to 0 is allowed in the chain. As the position of each node in the physical space is not explicitly specified in the stochastic model, a sequence of wet and dry nodes of this type is consistent with a stream network in which the active reaches, during wetting, expand either upstream or downstream (Durighetto et al., 2020). Furthermore, the hierarchical scheme is also suited to describe active networks that are not continuous in the physical space because of nonmonotonic changes of the local persistency along the network (see Figure 3 and section 5). Under the above assumptions, Equation 4 can be simplified as follows:

$$p(\boldsymbol{x}) = p_{000,\dots,0}^{[\prod_{j=1}^{N}(1-x_j)]} p_{100,\dots,0}^{[x_1\prod_{j=2}^{N}(1-x_j)]} p_{110,\dots,0}^{[x_1\ x_2\ \prod_{j=3}^{N}(1-x_j)]}, \dots, p_{111,\dots,1}^{[\prod_{j=1}^{N}x_j]}. \tag{15}$$

The transition between 1 and 0 in the chain is observed between the nodes $i-1$, i with a probability equal to $p_{10} = p_{i-1} - p_i$. Accordingly, the probability of a sequence of N consecutive active nodes is the probability that the least persistent node of the network is active, p_N. Likewise, the probability of a sequence of N consecutive dry nodes is the probability that the first node of the chain is dry, $1-p_1$. Therefore, the joint pdfs of all the possible combinations of states appearing in Equation 15 can be expressed as

$$\begin{aligned} p_{000,\dots,00} &= 1-p_1 \\ p_{100,\dots,00} &= p_1-p_2 \\ p_{110,\dots,00} &= p_2-p_3, \\ &\dots, \\ p_{111,\dots,10} &= p_{N-1}-p_N \\ p_{111,\dots,11} &= p_N. \end{aligned} \tag{16}$$

Provided that the geometry of the stream network is described by the active lengths associated to each node, the active stream length in this case only depends on the number of nodes active at a given time. Let us define L_i as the partial sum of the first i components of the vector $\boldsymbol{\Delta l}$, that is,

$$L_i = \sum_{k=1}^{i} \Delta l_k,\ (i \geq 1), \tag{17}$$

whereas $L_0 = 0$ by convention. L_i ($i = [0,1,2,\dots,N]$) identifies the length of the stream network when i nodes are active—only the nodes with persistency larger than (or equal to) p_i. This instance is observed with probability $p_{i-1} - p_i$ for $0 < i < N$ (see Equation 16). Therefore, a general expression for the pdf of the stream length can be written as

$$p_L(L) = \sum_{i=0}^{N} (p_i - p_{i+1})\delta(L - L_i), \tag{18}$$

where $\delta(\cdot)$ is the Dirac-delta generalized function (ref), $p_0 = 1$ and $p_{N+1} = 0$ to simplify the notation. The SLDC can then be calculated by means of Equation 7, or simply integrating the stream length pdf shown in Equation 18 as

$$P_L(L)=\int_0^L \sum_{i=0}^{i=N}(p_i - p_{i+1})\delta(x - L_i)dx=\sum_{i=0}^{i=N}(p_i - p_{i+1})H[L - L_i], \quad (19)$$

where $H(\cdot)$ is the unit Heavyside step function. Equation 19 is a linear stepwise function of L, and it can be rewritten as

$$P_L(L_i)=1 - p_i. \quad (20)$$

The right-hand side of Equation 20 expresses the cumulative probability of the local persistency along the network. Therefore, under the assumptions made, the SLDC can be seen as the spatial integral of the local persistency. This means that the duration of a given length (say, L^*) is the exceedance probability of the local persistency (interpreted as a spatial random variable) up to a suitable persistency threshold $p^*(L^*)$. This threshold is set in a way for which L^* is the overall network length when only the nodes with persistency larger than (or equal to) p^* are simultaneously switched on. Equation 20 suggests that the temporal distribution of the active stream length is linked to the spatial distribution of the local persistency. This space-for-time substitution for the estimation of the SLDC is allowed only when each node of the network constraints the status of the node(s) with a smaller persistency according to the hierarchical model.

3. Methods

The analysis of the major statistical and physical determinants of the shape of the SLDC is undertaken using observational data about the expansion/contraction dynamics of a real-world river network and a set of numerical Monte Carlo simulations of synthetic Bayesian networks.

3.1. Sensitivity Analysis With Synthetic Applications

The Monte Carlo simulations of synthetic networks consisted of a sequence of different steps, as detailed below. First, the configuration of a simulation was defined by specifying the structure of the network and the underlying statistical properties of the nodes. A Bayesian network is a Directed Acyclic Graph, in which each connection between couples of nodes has a direction (such that the parent and the child nodes can be identified, see section 2.2). Each node can be characterized by a single child or several children nodes, thereby allowing for the specification of a variety of network structures that include the following end-members: (i) a chain, in which each node has only one child; (ii) a tree with a single root node (i.e., a node without a parent), in which all the other nodes are directly connected to the one common parent. The structure is thus identified by assigning the connections among the nodes (parents and children). Afterward, the local persistency of the network nodes and their correlations with the direct parents $\rho_{i-1,i}$ were sampled from prescribed, independent pdfs. Different configurations were used to explore the impact of network structure, local persistency, and spatial correlation on the shape of the SLDC.

For each configuration, 10^5 Monte Carlo realizations of the states of the nodes were performed, and the length of the active streams was calculated for each realization. For the sake of simplicity, all the simulated networks consisted in 1,000 nodes, to each of which we assigned a unit length ($\Delta l_i = 1$). Then, for each configuration, 100 replicates of networks characterized by the same structure but a different population of correlations and local persistencies were generated and simulated. This made the resulting analysis independent on the specific samples of p_i and $\rho_{i-1,i}$ contained within each network.

Finally, the Monte Carlo realizations were used to calculate the pdf of the active stream length, its CDF (i.e., the SLDC) and the related moments. For the first two moments, the values obtained from the Monte Carlo simulations were compared to the corresponding analytical expressions (Equations 5 and 6), to exclude the presence of possible biases in the numerical simulations.

Even though in the simulations of the synthetic networks a standard unit length was associated to each node, our results could be easily extended to the general case of $\Delta l_i \neq const$, provided that each p_i is properly weighted with the corresponding Δl_i in the calculation of the mean petsistencies and correlations.

The degree of branching of the network was defined as the number of nodes in the network with more than one child. Starting from a linear chain, several synthetic networks with a prescribed degree of branching were obtained by reassigning a random parent to a subset of randomly selected nodes. The bigger the

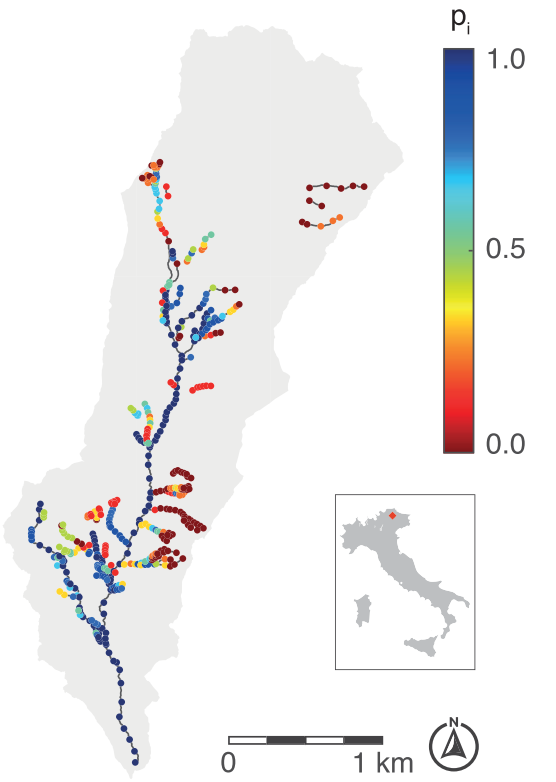

Figure 4. Bayesian network of the Valfredda river, northern Italy. Each node is colored on the basis of local persistency.

number of nodes belonging to this subset, the more branched the resulting network. This technique ensures that the length of individual network branches is exponentially distributed, in line with observational data (Convertino et al., 2007). To eliminate the possible effect of the specific structure of the network on the active length distribution, 100 different networks were simulated for each degree of branching. Then, we analyzed the full range of active length statistics obtained across the diverse tested configurations.

3.2. Application of the Model to a Study Catchment

The analysis also exploited observational data about stream network dynamics of the Valfredda river, a headwater stream in the Alps of northern Italy (Figure 4). The catchment has a drainage area of 5.3 km^2, and its altitudes range from 1,500 to 3,000 m above sea level. Local lithology, land cover, and geomorphology are spatially heterogeneous. This generates a dynamical stream network with a broad range of local persistencies and correlations. The climate of the area is Alpine, with an average annual precipitation of 1,500 mm unevenly distributed throughout the year. In particular, the seasonality of climate is reflected into short rainy summer and long snowy winters. The active stream network was monitored through 10 biweekly surveys from July to November 2018, encompassing different hydrological conditions. The surveys were carried out scouting each potential reach of the network and then recording the status of each network node and the underlying GPS node coordinates. A total of 16.8 km of network was observed, and 504 nodes with an average spacing of 30 m were used to characterize the spatial and temporal dynamics of the network. The specific location of each node was identified based on field surveys, so as to properly reproduce the geometrical complexity of the system. The definition of the nodes enabled the quantification of the hydrological conditions along the different stretches of the network based on the status of the reference nodes. The mean length of the stream reach associated to a nodes was 30 m, while the specific value for each node was estimated using a georeferenced high-resolution Digital Terrain Model. For more information about the study catchment and the field surveys, the reader is referred to Durighetto et al. (2020).

The experimental surveys were utilized to calculate the mean local persistency of each node in the observation period and the overall active length during each survey. These data were in turn used to check the reliability of the hierarchical model and for the estimate of the empirical SLDC in the Valfredda river, as detailed below.

For each survey, the observed active stream network was compared to the corresponding prediction of the hierarchical model. The latter consisted of a stream network map in which the nodes are switched on from the most persistent to the least persistent until the length of active streams observed during the considered survey is reached. Then, a confusion matrix was calculated to compare the observed and the modeled network, and the F_1 score was calculated as (Chinchor, 1992)

$$F_1=\frac{2TP}{2TP+FN+FP}. \tag{21}$$

In the above equation, *TP* (True Positive) quantifies the network length that the model correctly identifies as active, *FP* (False Positive) is the length that the model wrongly predicts as active, and *FN* (False Negative) is the length that the model wrongly predicts as dry. This score is a formal metric for assessing the accuracy of a binary classification, particularly when the classes are unbalanced (e.g., under dry conditions when almost all the network length is dry). The F_1 score ranges between 0 and 1, with the condition $F_1 = 1$ indicating the absence of errors in the classification.

The empirical SLDC in the Valfredda river was finally obtained from the observed length of the active streams during each survey via a plotting position (Leon Harter, 1983). This method consists in assigning a cumulative probability to each observed active stream length as

$$P_L(L)=\frac{r}{n+1} \tag{22}$$

where n is the number of surveys and r is the ordered rank of each surveyed length. This SLDC of the Valfredda river was compared with the cumulative exceedance probability of the local persistency along the network. The comparison was performed graphically and by means of the Mean Absolute Error (MAE) among the nine couples of available quantiles.

4. Results

This section describes the results of a series of numerical Monte Carlo simulations that were designed to disentangle the impact of the local persistency and its spatial correlation on the variability of the shape of the SLDC. The analysis is undertaken by first focusing on the simplified case of linear chains (sections 4.1and 4.2). Then the results are extended to branching networks (section 4.3). Finally, The robustness of the hierarchical model is tested using empirical data, and the features of the SLDC in a real-world case study are analyzed (section 4.4).

4.1. Impact of the Local Persistencies on the SLDC

The effect of the nodes persistency on the shape of the SLDC was explored in Figure 5 by comparing the results of a series of Monte Carlo simulations of six different network configurations. All the chains considered in Figure 5 share the same population of local correlations between directly connected nodes, $\rho_{i,j}$ (see caption of Figure 5). These chains differ in the spatial distribution of the local persistency across the nodes. In particular, the SLDCs shown in Figure 5b were obtained by sampling the local persistencies of the nodes from three beta distributions with a different variance and the same mean, as shown in Figure 5a. Likewise, three normal distributions with a mean persistency ranging between 0.25 and 0.75 and a constant variance (Figure 5c) were used to generate the SLDCs shown in Figure 5d.

Networks with the same mean persistency result in the same mean active stream length $\langle L\rangle$, regardless of the underlying spatial distribution of p_i, as shown in Figure 5b. Moreover, as suggested by Equation 5 and Figure 5d, $\langle L\rangle$ is directly proportional to $\langle p\rangle$. However, $\langle L\rangle$ does not depend on the spatial and temporal correlations of the status of the nodes, but only on their mean degree of persistency. This result stems from the definition of the total active length L (that is the sum of the lengths associated to each active node, see Equation 5), and from the mathematical definition of mean active length $\langle L\rangle$, which is here interpreted as the time average of L.

The variability of network length is quantified by the slope of the SLDC, which is proportional to the variance of L, $var(L)$. Intermediate local persistencies (i.e., $p_i = 0.5$) maximize the product $p_i(1-p_i)$ in Equation 6hence increasing the value of $var(L)$. Analogously, in Figure 5d, the SLDC that corresponds to the chain with a mean persistency equal to 0.5 generates a variance of L that is 35% higher than that obtained in the other two cases shown in the same panel (that correspond to a mean persistency of 0.25 and 0.75). Accordingly, a decrease of $var(L)$ can be observed, for a fixed mean persistency along the network of 0.5, when the variance of p across the different nodes increases, an instance that reduces the relative frequency of the nodes with intermediate persistencies. This is shown in Figure 5b, where the slope of the SLDC that corresponds to the smallest spatial variability of p is significantly higher than the slope of the *SLDC* obtained in the other cases. Note that the spatial variability of p along the network may also introduce significant constraints in the mutual correlations between nodes (see section 2.2), further reducing the variance of L (see 4.2).

4.2. Impact of the Local Correlations on the SLDC

The shape of the SLDC is influenced by the local correlations of the node states. The analysis is based on the results of the Monte Carlo simulation of six different network configurations, in which all the local persistencies were extracted from the same beta distribution (see caption of Figure 6). The underlying local

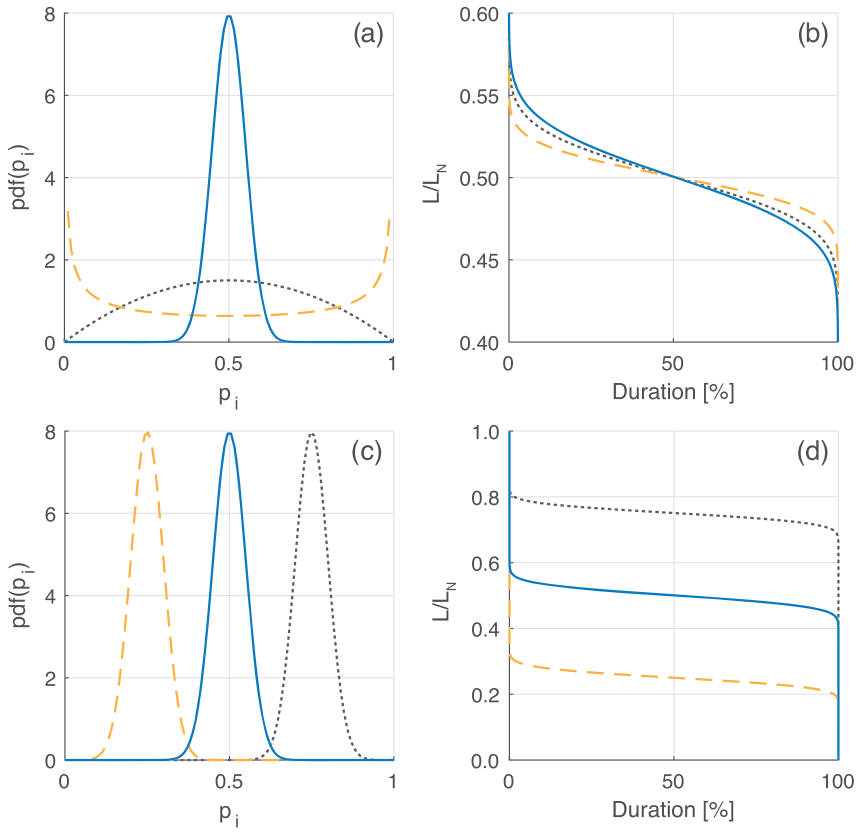

Figure 5. Length duration curves (panels b and d) obtained from chains of 1,000 nodes, with local persistencies extracted from the corresponding probability density function of panels (a) (beta distributions with $\langle p_i \rangle = 0.5$) and (c) (normal distributions with different means). Correlation between directly connected nodes are all extracted from a normal distribution with mean equal to 0.5. The $\langle L \rangle$ depends only on $\langle p_i \rangle$, while the $var(L)$ and the shape of the SLDC depends on the variability of the local persistency.

correlations, instead, were extracted from six different frequency distributions with heterogeneous means and/or variances, as shown in Figures 6a and 6c.

The three SLDC obtained starting from three different normal distributions of the local correlation (with a mean local correlation of 0.25, 0.50, and 0.75, see Figure 6a) are compared in Figure 6b. The resulting mean degree of correlation of the network in the three cases is 0.0017, 0.0030, and 0.0071, respectively. Higher $\langle \rho_{ntwk} \rangle$ produce steeper SLDCs and, consequently, a higher variability of L, as shown by the SLDCs in Figure 6b (and predicted by Equation 6). The full distribution of the local correlation within the network nodes, instead, does not affect the shape of the SLDC, if $\langle \rho_{ntwk} \rangle$ is constant. Accordingly, the three SLDCs reported in Figure 6d, which were obtained from three different distributions of the local correlation (see panel c) sharing the same mean network correlation are perfectly overlapped.

The combined effect of different local persistencies and local correlations on the SLDC is shown in Figure 7. Two different normal distributions for the local persistency (reported in Figure 7a) and two normal distributions for the local correlations (Figure 7b) were tested, and the four resulting SLDCs are shown in Figure 7c. Higher correlations are associated to steeper SLDCs, leading to an enhanced temporal variability of the active stream length. In fact, the two SLDCs that were obtained with the highest correlations (dashed lines) display a variance of L that is about 4 times bigger than that obtained for a lower value of the local correlations (solid lines). The effect of the local persistency on the slope of the SLDC, instead, is more limited, as the use of intermediate persistencies (blue lines) produce an increase in $var(L)$ of only 35% with respect to the cases in which the local persistencies are higher (yellow lines). These results also indicate that networks where intermediate persistencies are associated to high correlations are characterized by the steepest SLDCs.

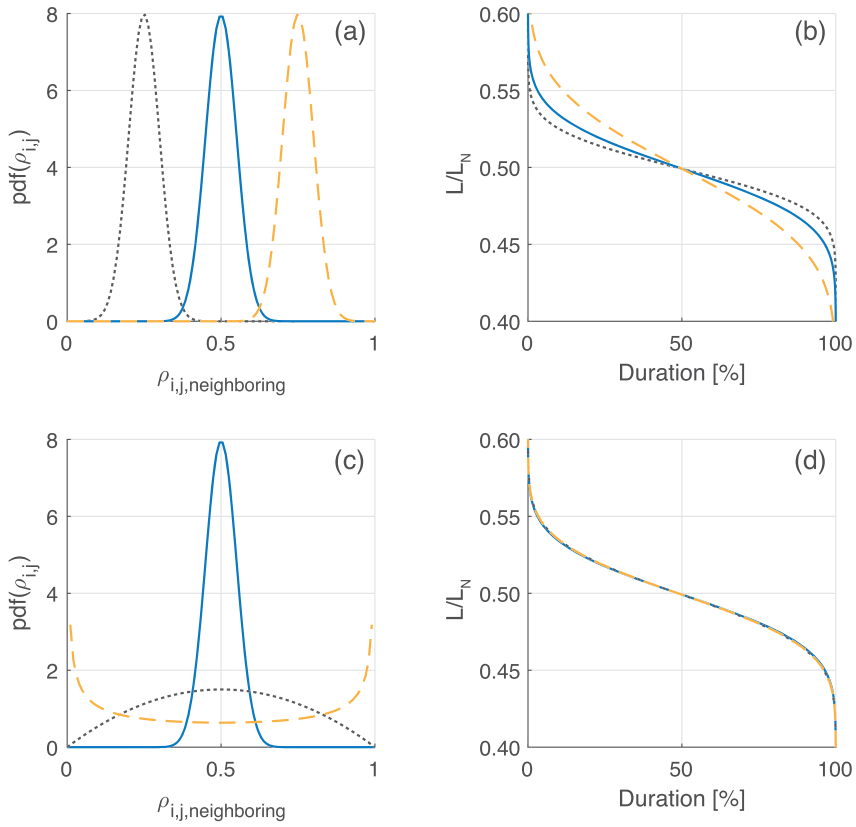

Figure 6. Length duration curves (panels b and d) obtained from chains of 1,000 nodes, with local persistencies extracted from a normal distribution with shape parameters $a = b = 50$, and an average of 0.5. The local correlations were sampled from the three normal distributions shown in panel (a) (with $\langle p_i \rangle = 0.25,0.5$, and 0.75) and from the three beta distributions represented in panel (c) (with $p_i = 0.5$). The shape of the SLDC (and consequently the variance of L) depends on the average correlation among the nodes but does not depend on the particular spatial distribution of ρ.

4.3. Impact of the Network Structure on the SLDC

The effect of the degree of branching of the network on the SLDC and the temporal variability of the active length is shown in Figure 8. The results of the simulations shown in the Figure are obtained starting from a single chain with a predefined configuration, as detailed in section 3.1 (see also caption of Figure 8).

An increase in the degree of branching of the network produces an increase of the variance of the active length $var(L)$, as shown in Figure 8a. In fact, for a given set of local persistencies and correlations, the smaller

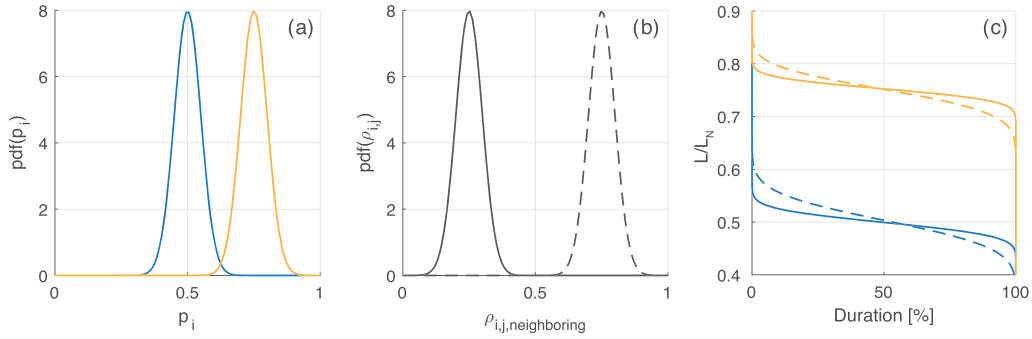

Figure 7. Length duration curves (panel c) obtained from chains of 1,000 nodes, with local persistencies extracted from the corresponding normal distribution of panel (a) and correlation between directly connected nodes extracted from the corresponding normal distribution of panel (b). Intermediate local persistencies increase $var(L)$ of a factor 1.35, while higher correlations increase $var(L)$ of a factor 4.2.

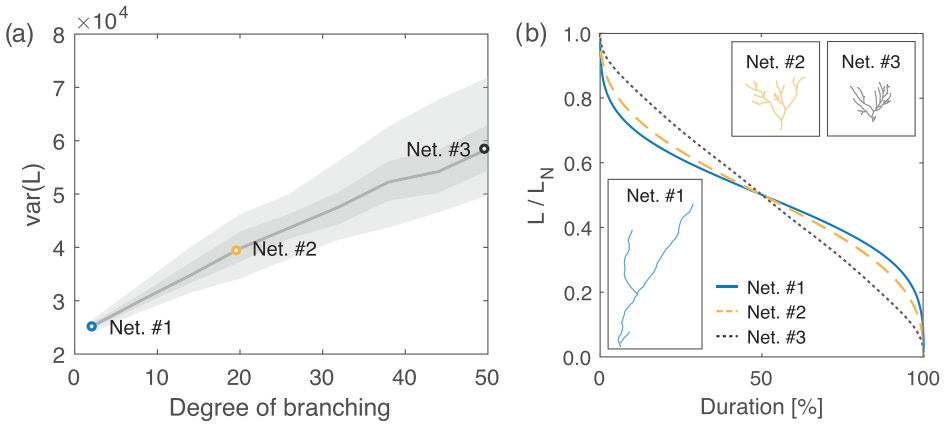

Figure 8. Variance of the active length as a function of the degree of branching (a), and length duration curves of 3 networks with different structures (b). All the simulations were performed on networks composed of 1,000 nodes, with local persistencies of 0.5 and correlations between directly connected nodes of 0.98. The light and dark shaded areas represent the 5th to 95th and 25th to 75th percentile ranges. The effect of network branching is to decrease the average distance between the nodes, thereby increasing ρ_{ntwk}. Therefore, more branched networks originate steeper SLDCs and a higher variability of the active length.

average distance between the nodes implied by a branching network ensures a higher correlation between the nodes that are not directly connected (see Equation 10) and, consequently, a higher value of $\langle\rho_{ntwk}\rangle$. This is reflected by higher values of $var(L)$ and a steeper SLDC, in agreement with the results shown in section 4.2. Networks with a higher degree of branching also present a wider range of possible values of $var(L)$ (Figure 8a), because of the higher number of different spatial configurations that can arise in river networks characterized by a larger number of tributaries.

Three examples of networks with different degrees of branching and their corresponding SLDC are shown in Figure 8b. The plot shows that, as the degree of branching increases, the SLDC is steeper—mirroring an increase in the temporal variability of the active length.

This monotonic relationship among the degree of branching, the network-scale correlation and the variance of L was found to be systematic, although its magnitude might depend on the underlying values of local persistency and correlation. In particular, the dependence of $var(L)$ on the network structure is stronger when the local correlations are higher, particularly if the integral scale of the process is larger than the mean distance between branching nodes (see section 5).

4.4. The Hierarchical Model and the SLDC of the Valfredda Catchment

The hierarchical model developed in section 2.3 is based on the assumption that the activation of the network nodes takes place in a hierarchical way, from the most to the least persistent. The validity of this hypothesis was tested using empirical data collected in the Valfredda catchment (see section 3). The bar plots of Figure 9a show, for each of the nine field survey performed in 2018 within the study catchment, how the observed active stream length is distributed among the different classes of local persistency (blue and red bars). Similarly, the gray and yellow bars represent the different classes of local persistency of the dry stream reaches during each survey. If the hypothesis of hierarchical activation was fulfilled, the persistency of the active reaches should be higher than the persistency of all the dry reaches. For each field survey, the length of the stream reaches that does not comply with the results predicted by the hierarchical model is shown in Figure 9 as yellow and red histograms. In particular, the yellow shading indicates the length of the reaches that the hierarchical model incorrectly predicts as active given the observed active stream length, while the red shading represents the length of the reaches that the model incorrectly predicts as dry.

The error produced by the hierarchical model in reproducing the observed stream network dynamics of the Valfredda catchment is very small (on average less then 3%, see Figure 9a). The performance of the hierarchical model was formally assessed via the F_1 score, which has an average value of 0.98. In the worst case (central plot in Figure 9a, with $F_1 = 0.96$), the overall length of the reaches that do not comply with the

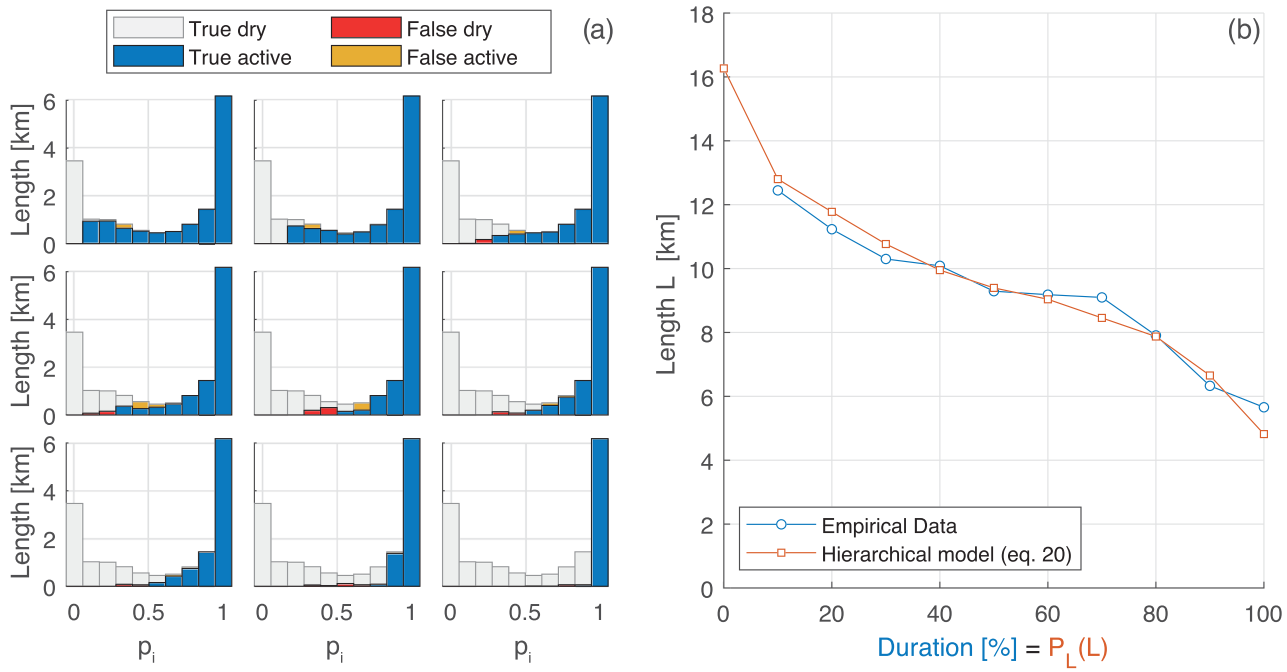

Figure 9. (a) Performance of the hierarchical model for the nine field surveys. Network length is classified by local persistence, and the predicted status from the hierarchical model is compared with the empirical data. The nine plots in panel (a) refer to different surveys, ordered from the wettest (top left) to the driest (bottom right). The smallest *F* score is 0.96. (b) Empirical SLDC of the Valfredda catchment obtained with the plotting position method (blue), compared with the cumulative probability of the local persistency along the network (orange).

hierarchical hypothesis is 500 m out of 16.8 km, while in the other cases this length decreases below 300 m. Interestingly, the error of the hierarchical model is smaller for very long or short river networks (top and bottom plots) and increases during intermediate wetness conditions of the catchment (middle plots).

The comparison between the empirical SLDC of the Valfredda catchment, which was obtained based on the field surveys performed in the summer and fall of 2018, and the prediction of the hierarchical model, that is, the cumulative exceedance probability of the local persistency along the network (Equation 20), is reported in Figure 9b. The two curves display a very similar behavior, with a MAE between the quantiles of 0.32 km. This confirms that spatial and temporal variability of streams are tightly linked, thereby allowing the calculation of the SLDC as the cumulative exceedance probability of the mean persistency of the different network nodes.

The SLDC embeds important information about the dynamics of the active stream network induced by climatic variability. The value of the active stream length with a duration of 100% corresponds to the length of the permanent streams of the network, which, according to the empirical observations, for the Valfredda river is about 5 km. The difference between the maximum and minimum length, instead, is the total length of the intermittent streams, approximately 11 km for this study catchment. About 4.5 km of temporary network is active more than 50% of the time. The median length (9.3 km, corresponding to a duration of 50%) is very similar to the mean length (9.2 km; see Durighetto et al., 2020), suggesting that the distribution of active stream lengths is not significantly skewed. In the range of durations between 10% and 90%, the slope of the SLDC is pronounced and uniform, thereby implying that the whole stream network is very dynamical, and there are no preferential values of the active length that are observed with a particularly high probability. The predicted increase in the slope of the SLDC for durations below 10% also suggests that a considerable length of stream network (3.5 km) is activated only during extremely wet climatic conditions.

5. Discussion

Developing theoretical tools suited to quantify the effect of unsteady climate drivers on the temporal variability of the active stream length might be pivotal to make a synthesis of available experimental data

gathered in different regions of the World and classify water courses based on the degree of persistency of their stretches. In this context, the concept of SLDC—the inverse of the exceedance probability of the total length of active streams—represents a flexible and simple mathematical tool that can be used by scientists and policy makers to characterize the temporal variability of the active fraction of the network, providing a benchmark for the assessment of the impact of stream network dynamics on a range of important hydrological, ecological and biogeochemical processes.

5.1. Drivers of the SLDC

Our analysis shows that the mean length of a dynamical network is proportional to the mean degree of persistency of its nodes, per se an extensive and site-dependent hydrological feature. From Equation 5, in fact, it follows that if we assume equally spaced nodes (i.e., $\Delta l_i = const$): $\langle L \rangle = \langle p \rangle L_N$, where L_N is the length of the stream network during its maximum expansion (see Equation 17) and $\langle p \rangle$ is the mean persistency of all the nodes. This result indicates that the average length of the actively flowing streams is only affected by the local mean status of the different nodes, without being impacted by the underlying spatial and temporal patterns of network expansion (contraction) during wetting (drying). Consequently, flashy streams, which experience frequent expansion and contraction cycles in response to individual events, may display the same mean active length exhibited by streams with slower seasonal dynamics.

The slope of the SLDC, instead, is a measure of the temporal changes in the length of the active stream network, as induced by the underlying hydrological variability. Our results indicate that intermediate persistencies and high correlations among the states of the network nodes tend to promote the temporal variability of the length of the active streams. Consequently, we expect the effect of the expansion and contraction cycles experienced by river networks on the temporal patterns of the length of active streams to be reduced under very humid and very arid conditions, where the local persistencies of the network nodes might approach the limiting values of unit and zero (Costigan et al., 2016; Ward et al., 2018). Furthermore, this result indicates that an increase in the spatial correlation of the underlying hydrological drivers during the activation of temporary reaches should enhance the observed temporal changes in the overall network length by increasing the correlation of the status of the nodes. Note, however, that a constant length of the active streams (i.e., a stepwise SLDC) does not imply the lack of any stream network dynamics. In fact, poorly correlated spatial dynamics of river networks could potentially generate nearly constant active lengths.

Our results also reveal that, for a given distribution of local persistencies and local correlations, the presence of branching river networks tends to increase the overall spatial correlation of the states of the network nodes. Consequently, *ceteris paribus*, the temporal variability of the length of the active streams is higher for branching streams, because the information about the state of each node has the opportunity to propagate faster and more efficiently to the other nodes of the network. Therefore, during wet periods, the temporal variability of the active stream length is expected to be higher than that observed during dry periods, when the mean drainage density is lower. The increase of the temporal variability of the active stream length associated with branched network structures is more significant when the underlying node correlations are higher, so as the integral scale of the stochastic process that defines the states of the nodes is larger than the mean distance between two nearest branching nodes. In fact, as suggested by Equation 10, the correlation between two nodes decreases as their distance increases. Accordingly, when the local correlations are small, the overall network correlation drops-off and becomes roughly independent on the underlying network structure. For instance, in the Valfredda river, the observed mean correlation of the dynamical fraction of the network is 0.6. Under these circumstances, the effect of the network structure on the shape of the SLDC proved to be less important than that produced by other factors, such as the distribution of the local persistency and its correlation.

The numerical simulations performed using synthetic networks enable the identification of the full hierarchy of controls on the main probabilistic features of the active length in intermittent watercourses. The most important statistical property that drives the dynamics of the active fraction of temporary streams is the local persistency of the nodes that affects both the mean and the variance of L. The local correlation, instead, acts as a second-order control of the *SLDC*, in that low network correlations tend to decrease $var(L)$, as per Equation 6. Finally, the degree of network branching is the least important driver of the *SLDC*, as network structure matters only when the mean network correlation is particularly high.

It is worth mentioning that the *SLDC* is a flexible statistical index that can be used to describe active length variations over a broad range of timescales, from single events to full seasons or years. The reference temporal scale of the *SLDC*, in fact, can be arbitrarily defined depending on the hydrological processes of interest (e.g., storm dynamics, seasonal wetting-drying cycles, and interannual hydroclimatic fluctuations), possibly taking into account the temporal resolution of available data for the estimation of the local perisitencies throughout the network (see section 5.3). Analogously, the *SLDC* enables the description—and possibly also the comparison—of active stream dynamics at different spatial scales, from small headwater catchments to large rivers. The main constraint associated to the application of this approach to large spatial scales is the huge empirical effort required for the monitoring of network dynamics in large river basins (but see section 5.3).

Overall, our results show that the SLDC is able to summarize the extent and variability of a dynamical stream integrating the effect of diverse hydrological features of its nodes. The average active length is represented by the area below the *SLDC*, while the extent of the maximum (i.e., potential) and the permanent networks are quantified by the active lengths that correspond to a duration of 0% and 100%, respectively. Accordingly, the *SLDC* of a temporary stream that completely dries out for some time during the year should be characterized by a distinctive intersection with the x axis for $D < 1$. Instead, the slope of the curve quantifies in a graphical manner the magnitude of network dynamics, with higher slopes in the *SLDC* indicating a higher variability of the active length. Likewise, heterogeneous slopes across different durations ranges suggest the presence of spatial and temporal heterogeneities in network dynamics, originated, for example, by the simultaneous presence of multiple preferential frequencies in the expansion and contraction cycles of temporary streams.

For the above reasons, we believe that the *SLDC* may be a useful tool to effectively characterize the extent and variability of the active network in rivers, providing a basis to quantitatively compare stream dynamics across different climatic regions and objectively classify temporary rivers.

5.2. Hierarchical Activation of the Stream Network

The empirical estimate of the SLDC of the Valfredda river (Italy) during the summer and fall of 2018 revealed that the SLDC of a humid headwater catchment located in the Alpine region can be quite steep and regular, thereby evidencing a pronounced and constant sensitivity of the length of active streams to the underlying hydrological conditions. Biweekly empirical data collected in the Valfredda catchment also indicates that the activation of the different stretches of the river network during the study period follows a systematic order in which the most persistent stretches are activated first, while the least persistent reaches are active only when the river network is fully expanded. This implies that the activation of nodes during wetting always follows a predefined order, dictated by their persistency, and the subsequent network contraction follows the inverse order (i.e., the last parts of the network that become active are also the first to dry out). The observed dynamics of the active length in the Valfredda catchment were found to correlate with the 5 and 35 days antecedent precipitation, suggesting that this hierarchical behavior holds within single storm events and seasonally (Durighetto et al., 2020). Whereas more data would be needed to verify the generality of this hierarchical activation rule under different field conditions (e.g., climate, geology, and catchment size), the potential implications of this phenomenon for the mapping and the modeling of stream network dynamics are manyfold.

First of all, when the activation of temporary streams is hierarchical the temporal variability of the stream length, as quantified by the SLDC, corresponds to the spatial CDF of the local persistency (space-for-time substitution). This means that under ergodic conditions, different portions of the network could be surveyed during disjoint periods to estimate the spatial patterns of p_k (Equation 2) and then this information could be used to estimate the SLDC at larger scales. This is feasible because the hierarchical hypothesis postulates that the activation of nodes with the same local persistency is synchronous. Therefore, if the local persistencies of different portions of a whole network are known, the behavior of some nodes can be reconstructed from synchronous observations about the status of other nodes. As the full-mapping of the active streams is highly time-consuming even in relatively small rivers—and almost impractical for larger catchments—the space-for time substitution implied by the hierarchical behavior of temporary streams would enhance our ability to estimate the observed changes of the stream network length in relatively large rivers.

Second, the hierarchical activation/deactivation of temporary streams according to their mean persistency establishes a one-to-one relationship between the total length of the active streams and the spatial pattern of active streams, provided that the mean local persistency of each node can be independently estimated. This could be useful to interpolate observed active stream maps through time, and to extrapolate in space the available surveys of flowing streams (e.g., exploiting the assumption that all streams with the same persistency are simultaneously activated and deactivated, see section 2.3).

Finally, the hierarchical scheme of stream expansion is a possible indirect manifestation of causality in the activation/deactivation of temporary network stretches. According to the hierarchical scheme, the activation of a reach with a high persistency is a necessary but not sufficient condition for the activation of all the stretches with a lower persistency. Therefore, the validity of the hierarchical scheme suggests the presence of a hydrological signal that propagates during wetting from the most humid sites of the catchment (that host the most persistent streams) to the least humid areas (where the most temporary streams are located). The hierarchical scheme is compatible with the concept of Variable Source Areas (VSA), which predicts a progressive expansion of saturated areas around the permanent river network during wetting (Bernier, 1985; Hewlett & Hibbert, 1967; Hibbert & Troendle, 1988); however, while the VSA concept typically originates connected river networks, this is not necessarily true for the hierarchical activation model of temporary tributaries in dynamical river networks. In fact, the degree of persistency of the different nodes might not be a monotonic function along a given flow path, as local disconnections can be observed in response to heterogeneity of topographic and soil features (see Durighetto et al., 2020). Under these circumstances, the hierarchical model generates dynamically disconnected stream networks. This is in line with the presence of dynamic stream networks generated by a shallow water table that raises and falls within a complex topographic and geologic setting, depending on the underlying hydrological conditions, and intersects different portions of the landscape (Bertassello et al., 2019; Costigan et al., 2016). A systematic hierarchical activation driven by the underlying persistency is, instead, not compatible with the presence of marked internal heterogeneity in the input climatic signal, which would lead to the selective activation of diverse portions of the stream network, regardless of their mean degree of persistency. This selective activation of different reaches in response to heterogeneous forcing, would reduce the spatial correlation of the nodes states, breaking the one-to-one relationship between the overall length of the active streams and the persistency of active nodes. Consequently, the assumption of hierarchical activation of the temporary streams of the network would not hold any longer. Our data seems to suggest that such internal climatic heterogeneity is not the main driver of the observed stream network dynamics in the Valfredda catchment. Nevertheless, more research with a bigger data set is necessary to properly constrain the spatial and temporal scales within which the activation and contraction of temporary streams is hierarchical in other contexts.

5.3. Limitations and Prospects

In spite of the generality of the analytical derivations of this paper, it is worth highlighting that the theoretical tools developed in this paper are purely statistical. As such, they have limited predictive power, unless they are properly complemented by physically based models able to uncover the major physical determinants of the spatial patterns of stream persistency and its correlation. Another important limitation of the approach is that only temporally averaged statistics of the active length are investigated, while all the temporal correlations of network dynamics are not analyzed. Furthermore, the approach itself is intrinsically demanding from the viewpoint of the data that are necessary for its application and implementation. In fact, the key element of the whole theory is the local persistency of the network nodes, which needs to be estimated from empirical surveys of the active portion of the network due to the current lack of predictive models of stream dynamics. As the local persistency is the sample mean of the status of each node (see Equations 1 and 2), these field surveys should be independent and in sufficient number to ensure a reasonable representation of the network dynamics at the temporal scales of interest. The number of empirical surveys proves crucial not only to constrain the minimum frequency of network dynamics that can be captured by the *SLDC* (roughly, the mean interarrival between the surveys) but also to set the number of different quantiles available in the empirical *SLDC*. On this basis we hypothesize that about 5 to 10 independent surveys should be a minimum requirement for constructing a reliable SLDC at intra-annual timescales. For longer periods, instead, the above numbers are likely to generate a significant underestimation of the event-based variability of the active network. Nevertheless, the reliability of empirical estimates of p can be enhanced if the field

surveys are informed by available rainfall or stream flow data (Durighetto et al., 2020; Jensen et al., 2017). Moreover, the operational efforts associated to the mapping of active streams could be significantly reduced if the mathematical properties of the hierarchical activation of temporary streams are exploited, provided that the status of some nodes can be deduced from the status of other nodes in the network. Ongoing research is also devoted to develop modeling tools for estimating the local persistency with the support of climatic and physiographic features. Such models could be very helpful to further reduce the empirical efforts necessary to estimate the persistencies of the nodes in temporary river networks.

In spite of the above limitations, and the data-demanding nature of the proposed approach, we believe that the framework developed in this paper provides a strong basis to define general and objective metrics for the quantification river network dynamics and offer useful insights on the complex relationship between local and catchment-scale network attributes of temporary streams.

6. Conclusion

In this paper we have developed a stochastic framework suited to objectively quantify the impact of unsteady climatic drivers on the length of the active flowing network. In particular, we have proposed and formalized the concept of SLDC, a novel hydrologic index that can be used to summarize efficiently the effect of hydrological variability on the extent of the flowing stream network under a variety of climatic conditions and field settings. A stochastic model has been developed to link the shape of the SLDC to the local persistency of the stream network nodes and its spatial correlation. The theoretical and empirical analysis carried out in this contribution brought us to formulate the following key conclusions:

1. The mean length of the stream network is solely dictated by the mean persistency of the different nodes of the stream network. The higher the overall average of the node persistencies, the higher the mean length of the active streams and the area of the SLDC.
2. The shape of the SLDC, instead, is driven by the pdf of the local persistencies and, to a lesser extent, their network-scale spatial correlation. In particular, intermediate persistencies and highly correlated states enhance the network length dynamics, thereby implying steeper SLDCs. Conversely, low or high persistencies, and poorly correlated states smooth the changes of the active stream length through time, and originate nearly horizontal SLDCs.
3. The presence of branching river networks enhance the overall network-scale correlation, especially when the integral scale of the nodes states is higher then the mean distance between two subsequent tributaries. This circumstance in turn increases the active network length variability, originating steeper SLDCs.
4. The SLDC of the Valfredda river was estimated based on 10 field surveys conducted during the summer and fall of 2018. The SLDC of this humid headwater catchment of the Italian Alpine region is quite steep and regular, with an average slope of 1 km for percentile. This reflects a pronounced sensitivity of the length of active streams to the underlying hydrological conditions.
5. Observational data also suggest that the activation of the different stream reaches during network expansion in the Valfredda river is systematically hierarchical, from the most persistent to the least persistent nodes. The same applies during the network contraction that proceeds from the most temporary to the least temporary stream reaches of the network. This hierarchical activation of the reaches of the stream network is possibly a reflection of causality (i.e., presence of common hydrological drivers in the contributing catchment).
6. When the activation of the stream network is hierarchical, as described above, the state of the network nodes is highly correlated and the temporal variability of the network length is enhanced; under these circumstances, the SLDC corresponds to the spatial CDF of the persistency of the different nodes in the network (i.e., space for time substitution is allowed).

This study provides a basis for the development of comparative studies of stream network dynamics across different climatic regions and offers a clue for the development of stochastic and mechanistic models for the expansion and contraction of actively flowing streams.

Data Availability Statement

All the empirical data used in this study is publicly available, see citations in text.

Acknowledgments
This study was supported by the European Research Council (ERC) "DyNET" project funded through the European Community's Horizon 2020 —Excellent Science—Programme (Grant Agreement H2020-EU.1.1.-770999). We thank the editors and three anonymous reviewers for all the insightful comments on the paper.

References

Agren, A. M., Lidberg, W., & Ring, E. (2015). Mapping temporal dynamics in a forest stream network—Implications for riparian forest management. *Forests*, *6*(9), 2982–3001. https://doi.org/10.3390/f6092982

Arthington, A. H., Bernardo, J. M., & Ilhéu, M. (2014). Temporary rivers: Linking ecohydrology, ecological quality and reconciliation ecology. *River Research and Applications*, *30*, 1209–1215. https://doi.org/10.1002/rra.2831

Basu, N. B., Rao, P. S. C., Thompson, S. E., Loukinova, N. V., Donner, S. D., Ye, S., & Sivapalan, M. (2011). Spatiotemporal everaging of in-stream solute removal dynamics. *Water Resources Research*, *47*, W00J06. https://doi.org/10.1029/2010WR010196

Bernal, S., & Sabater, F. (2008). The role of lithology, catchment size and the alluvial zone on hydrogeochemistry of two intermittent Mediterranean streams. *Hydrological Processes*, *22*, 1407–1418. https://doi.org/10.1002/hyp.6693

Bernier, P. Y. (1985). Variable source areas and stormflow generation: An update of the concept and a simulation effort. *Journal of Hydrology*, *79*, 195–213. https://doi.org/10.1016/0022-1694(85)90055-1

Bertassello, L. E., Rao, P. S. C., Jawitz, J. W., Aubeneau, A. F., & Botter, G. (2019). Wetlandscape hydrologic dynamics driven by shallow groundwater and landscape topography. *Hydrological Processes*, *34*, 1460–1474.

Bertuzzo, E., Helton, A. M., Hall Jr, R. O., & Battin, T. J. (2017). Scaling of dissolved organic carbon removal in river networks. *Advances in Water Resources*, *110*, 136–146. https://doi.org/10.1016/j.advwatres.2017.10.009

Blyth, K., & Rodda, J. (1973). A stream length study. *Water Resources Research*, *9*(5), 1464–1461.

Botter, G., Porporato, A., Rodriguez-Iturbe, I., & Rinaldo, A. (2007). Basin-scale soil moisture dynamics and the probabilistic characterization of carrier hydrologic flows: Slow, leaching-prone components of the hydrologic response. *Water Resources Research*, *43*, W02417. https://doi.org/10.1029/2006WR005043

Butturini, A., Alvarez, M., Bernal, S., Vasquez, E., & Sabater, F. (2008). Diversity and temporal sequences of forms of DOC and NO_3−discharge responses in an intermittent stream: Predictable or random succession? *Journal of Geophysical Research*, *113*, G03016. https://doi.org/10.1029/2008JG000721

Castellarin, A., Galeati, G., Brandimarte, L., Montanari, A., & Brath, A. (2004). Regional flow-duration curves: Reliability for ungauged basins. *Advances in Water Resources*, *27*, 953–965. https://doi.org/10.1016/j.advwatres.2004.05.005

Chinchor, N. (1992). Muc-4 evaluation metrics. In *Proc. of the Fourth Message Understanding Conference* (pp. 22–29).

Convertino, M., Rigon, R., Maritan, A., Rodriguez-Iturbe, I., & Rinaldo, A. (2007). Probabilistic structure of the distance between tributaries of given size in river networks. *Water Resources Research*, *43*, W11418. https://doi.org/10.1029/2007WR006176

Costigan, K. H., Jaeger, K. L., Goss, C. W., Fritx, K. M., & Goebel, P. C. (2016). Understanding controls on flow permanence in intermittent rivers to aid ecological research: Integrating meteorology, geology and land cover. *Ecohydrology*, *9*(7), 1141–1153. https://doi.org/10.1002/eco.1712

Dai, B., Ding, S., & Wahba, G. (2013). Multivariate Beronulli distribution. *Bernoulli*, *19*(4), 1465–1483. https://doi.org/10.3150/12-BEJSP10

Datry, T., Boulton, A. J., Bonada, N., Fritz, K., Leigh, C., Sauquet, E., et al. (2017). Flow intermittence and ecosystem services in rivers of the Antropocene. *Journal of Applied Ecology*, *55*, 353–364. https://doi.org/10.1111/1365-2664.12941

Datry, T., Larned, S. T., & Tockner, K. (2014). Intermittent rivers: A challenge for freshwater ecology. *BioScience*, *64*(3), 229–235. https://doi.org/10.1093/biosci/bit027

Datry, T., Pella, H., Leigh, C., Bonada, N., & Hugueny, B. (2016). A landscape approach to advance intermittency river ecology. *Freshwater Biology*, *61*, 1200–1213. https://doi.org/10.1111/fwb.12645

Day, D. G. (1978). Drainage density changes during rainfall. *Earth Surface Processes*, *3*, 319–326.

Doering, M., Uehlinger, U., Rotach, A., Sclaepfer, D. R., & Tockner, K. (2007). Ecosystem expansion and contraction dynamics along a large Alpine alluvial corridor (Tagliamento River, Northeast Italy). *Earth Surface Processes and Landforms*, *32*, 1693–1704. https://doi.org/10.1002/esp.1594

Doulatyari, B., Betterle, A., Basso, S., Biswal, B., Schirmer, M., & Botter, G. (2015). Predicting streamflow distributions and flow duration curves from landscape and climate. *Advances in Water Resources*, *83*, 285–298. https://doi.org/10.1016/j.advwatres.2015.06.013

Downing, J. J., Cole, J. J., Duarte, C. M., Middelburg, J. J., Melack, J. M., Prairie, Y. T., et al. (2012). Global abundance and size distribution of streams and rivers. *Inland Waters*, *2*(4), 229–236. https://doi.org/10.5268/IW-2.4.502

Durighetto, N., Vingiani, F., L.E., B., Camporese, M., & Botter, G. (2020). Intra-seasonal drainage network dynamics in a headwater catchment of the italian alps. *Water Resources Research*, *56*, e2019WR025563. https://doi.org/10.1029/2019WR025563

Garbin, S., Alessi Celegon, E., Fanton, P., & Botter, G. (2019). Hydrological controls on river network connectivity. *Royal society open science*, *6*, 181,428. https://doi.org/10.1098/rsos.181428

Godsey, S. E., & Kirchner, J. W. (2014). Dynamic, discontinuous stream networks: Hydrologically driven variations in active drainage density, flowing channels and stream order. *Hydrological Processes*, *28*, 5791–5803.

Goulsbra, C., Evans, M., & Lindsay, J. (2014). Temporary streams in a peatland catchment: Pattern, timing, and controls on stream network expansion and contraction. *Earth Surface Processes and Landforms*, *39*, 790–803. https://doi.org/10.1002/esp.3533

Gregory, K. J., & Walling, D. E. (1968). The variation of drainage density within a catchment. *International Association of Scientific Hydrology Bulletin*, *13*, 61–68. https://doi.org/10.1080/02626666809493583

Hewlett, J. D., & Hibbert, A. R. (1967). Factors affecting the response of small watersheds to precipitation in humid areas. *Forest Hydrology*, *1*, 275–290.

Hibbert, A. R., & Troendle, C. A. (1988). Streamflow generation by variable source area. *Forest hydrology and ecology at Coweeta* (Vol. 1, pp. 111–127). New York, NY: Springer. https://doi.org/10.1007/978-1-4612-3732-7_8

Jaeger, K. L., Montgomery, D. R., & Bolton, S. M. (2007). Channel and perennial flow initiation in headwater streams: Management implications of variability in source-area size. *Environmental Management*, *40*, 775–786. https://doi.org/10.1007/s00267-005-0311-2

Jaeger, K. L., Olden, J. D., & Pelland, N. A. (2014). Climatae change poised to threaten hydrologic connectivity and endemic fishes in dryland streams. *Proceedings od the National Academy of Sciences*, *111*, 13,894–13,899. https://doi.org/10.1073/pnas.1320890111

Jensen, C. K., McGuire, K. J., McLaughlin, D. L., & Scott, D. T. (2019). Quantifying spatiotemporal variation in headwater stream length using flow intermittency sensors. *Environmental Monitoring and Assessment*, *191*, 191–226. https://doi.org/10.1007/s10661-019-7373-8

Jensen, C. K., McGuire, K. J., & Prince, P. S. (2017). Headwater stream length dynamics across four physiographic provinces of the Appalachian Highlands. *Hydrological Processes*, *31*, 3350–3363. https://doi.org/10.1002/hyp.11259

Jensen, C. K., McGuire, K. J., Shao, Y., & Dolloff, C. A. (2018). Modeling wet headwater stream networks across multiple flow conditions in the Appalachian Highlands. *Earth Surface Process and Landforms*, *43*, 2762–2778. https://doi.org/10.1002/esp.4431

Larned, S. T., Datry, T., Arscott, D. B., & Tockner, K. (2010). Emerging concepts in temporary-river ecology. *Freshwater Biology*, *55*, 717–738. https://doi.org/10.1111/j.1365-2427.2009.02322.x

Leon Harter, H. (1983). Another look at plotting positions. *Communications in Statistics - Theory and Methods*, *13*, 1613–1633. https://doi.org/10.1080/03610928408828781

Lovill, S. M., Hahm, W. J., & Dietrich, W. E. (2018). Drainage in the critical zone: Lithologic controls on the persistence and spatial extent of wetted channels during the summer dry season. *Water Resources Research*, *54*, 5702–5726. https://doi.org/10.1029/2017WR021903

Malard, F., Ueglinger, U., Zah, R., & Tockner, K. (2006). Flood-pulse and riverscape dynamics in a braided glacial river. *Ecology*, *87*(3), 704–716.

Marzadri, A., Dee, M. M., Tonina, D., Bellin, A., & Tank, J. (2017). Role of surface and subsurface processes in scaling N2O emissions long riverine networks. *Proceedings of the National Academy of Sciences*, *114*, 4330–4335. https://doi.org/10.1073/pnas.1617454114

McDonough, O. T., Hosen, J. D., & Palmer, M. A. (2011). Temporary streams: The hydrology, geography and ecology of non-perennially flowing waters. River Ecosystems: Dynamics, Management and Conservation, 259–289.

Peirce, S. E., & Lindsay, J. B. (2015). Characterizing ephemeral streams in a southern Ontario watershed using electrical resistance sensors. *Hydrological Processes*, *29*, 103–111. https://doi.org/10.1002/hyp.10136

Peterson, B. J., Wollheim, W. W., Mulholland, P. J., Webster, J. R., Meyer, J. L., Tank, J. L., et al. (2001). Control of nitrogen export from watersheds by headwater streams. *Science*, *292*, 86–90. https://doi.org/10.1126/science.1056874

Roberts, M., & Klingeman, P. (1972). The relationship between drainage net fluctuation and discharge. In Adams & Helleiner (Eds), *International Geography, Proceedings of the 22nd International Geographical Congress, Canada* (189–191). University of Toronto Press.

Sarremejane, R., Cañelles-Argüelles, M., Prat, N., Mykrä, H., Muotka, T., & Bonada, N. (2017). Do metacommunities vary through time? Intermittent rivers as model systems. *Journal of Biogeography*, *44*, 2752–2763. https://doi.org/10.1111/jbi.13077

Shaw, S. B. (2016). Investigating the linkage between streamflow recession rates and channel network contraction in a mesoscale catchment in New York state. *Hydrological Processes*, *30*, 479–492. https://doi.org/10.1002/hyp.10626

Shaw, S. B., Bonville, D. B., & Chandler, D. G. (2017). Combining observations of channel network contraction and spatial discharge variation to inform spatial controls on baseflow in Birch Creek, Catskill Mountains, USA. *Journal of Hydrology: Regional Studies*, *12*, 1–12. https://doi.org/10.1016/j.ejrh.2017.03.003

Skoulikidis, N. T., Sabater, S., Datry, T., Morais, M. M., Buffagni, A., Drflinger, G., et al. (2017). Non-perennial Mediterranean rivers in Europe: Status, pressures and challenges for research and management. *Science of the Total Environment*, *577*, 1–18. https://doi.org/10.1016/j.scitotenv.2016.10.147

Steward, A. L., von Schiller, D., Tockner, K., Marchall, J. C., & Bunn, S. E. (2012). When the river runs dry: Human and ecological values of dry riverbeds. *Frontiers in Ecology and the Environment*, *10*, 202–209. https://doi.org/10.1890/110136

Tooth, S. (2000). Process, form and change in dryland rivers: A review of recent research. *Earth-science reviews*, *51*, 67–107. https://doi.org/10.1016/S0012-8252(00)00014-3

van Meerveld, H. J. I., Kirchner, J. W., Vis, ARS, & Seivert, J. (2019). Expansion and contracion of the flowing network changes hillslope flowpath lengths and the shape of the travel time distribution. *Hydrological and Earth System Sciences*, *23*, 4825–4834. https://doi.org/10.5194/hess-2019-218

Vogel, R. M., & Fennessey, N. M. (1994). Flow-duration curves: New interpretation and confidence intervals. *Journal of Water Resources Planning and Management*, *120*, 485–504. https://doi.org/10.1061/(ASCE)0733-9496(1994)120:4(485)

Ward, A., Schmadel, N. M., & Wondzell, S. M. (2018). Simulation of dynamic expansion, contraction, and connectivity in a mountain stream network. *Advances in Water Resources*, *114*, 64–82. https://doi.org/10.1016/j.advwatres.2018.01.018

Whiting, J. A., & Godsey, S. E. (2016). Discontinuous headwater stream networks with stable flowheads, Salmon River basin, Idaho. *Hydrological Processes*, *30*, 2305–2316. https://doi.org/10.1002/hyp.10790

Wiginton, P. J., Moser, T. J., & Lindeman, D. R. (2005). Stream network expansion: A riparian water quality factor. *Hydrological Processes*, *19*(8), 1715–1721. https://doi.org/10.1002/hyp.5866

Zimmer, M. A., & McGlynn, B. L. (2017). Ephemeral and intermittent runoff generation processes in a low relief, highly weathered catchment. *Water Resources Research*, *53*, 7055–7077. https://doi.org/10.1002/2016WR019742